Journal of Virology, Mar. 1993, p. 1137–1147
0022-538X/93/031137-11$02.00/0

Vol. 67, No. 3

Correlation of Specific Virus-Astrocyte Interactions and Cytopathic Effects Induced by *ts*1, a Neurovirulent Mutant of Moloney Murine Leukemia Virus

E. SHIKOVA,[1] Y.-C. LIN,[1] KUNAL SAHA,[1] B. R. BROOKS,[2] AND P. K. Y. WONG[1]*

The University of Texas M. D. Anderson Cancer Center, Science Park—Research Division, Smithville, Texas 78957,[1] and Neurology Service, William S. Middleton Veterans Administration Hospital, University of Wisconsin, Madison, Wisconsin 53706[2]

Received 19 May 1992/Accepted 16 November 1992

***ts*1 is a highly neuropathogenic and lymphocytopathic mutant of Moloney murine leukemia virus TB (MoMuLV-TB). We previously reported that the primary neuropathogenic determinant of *ts*1 maps to a single amino acid substitution, Val-25→Ile, in precursor envelope protein gPr80*env*. This Val-25→Ile substitution apparently renders gPr80*env* inefficient for transport from the endoplasmic reticulum to the Golgi apparatus. These findings suggest that the cytopathic effect of *ts*1 in neural cells might be due to the accumulation of gPr80*env* in the endoplasmic reticulum. Since endothelial and glial cells are targets of *ts*1 infection in the central nervous system, we established primary endothelial and astrocyte cultures to investigate the mechanism of cell killing caused by *ts*1. A continuous cell line, TB, was used as a control. Our results showed that both *ts*1 and MoMuLV-TB replicated and induced a cytopathic effect in astrocyte cultures, albeit to different degrees; *ts*1 appeared to be more lethal than MoMuLV-TB. On the other hand, *ts*1 and MoMuLV-TB infections of endothelial or TB cells were not cytopathic. The cytopathic effect in infected astrocytes correlated with the inefficiency of gPr80*env* transport and the intracellular accumulation of gPr80*env* as well as aberrant virus particles.**

For the past several years, we have been studying the pathogenesis of a progressive spongiform encephalomyelopathy induced in mice by *ts*1, a highly neuropathogenic and lymphocytopathic mutant of Moloney murine leukemia virus TB (MoMuLV-TB) (33, 40). To understand the molecular and cellular events leading to the neurodegenerative disease induced by *ts*1, our main goal has been to determine the virus factor(s) responsible for disease induction and the mechanism of specific cell killing by the virus.

We previously reported that the primary neuropathogenic determinant of *ts*1 maps to a single amino acid substitution, Val-25→Ile, in precursor envelope protein gPr80*env* (29, 34). Under restrictive growth conditions, the Val-25→Ile substitution did not prevent the oligomerization of gPr80*env*. However, the gPr80*env* oligomer was inefficient for transport from the endoplasmic reticulum (ER) to the Golgi apparatus (15). It has been hypothesized that the cytopathic effect (CPE) of *ts*1 in neural cells might be due at least in part to the accumulation of the gPr80*env* oligomer in the ER (29, 40, 41). In in vivo studies, we found that the viral titer in the central nervous system (CNS) apparently correlates with the progression of neurologic disorders and that the degenerative changes in the CNS appear to be a direct consequence of virus replication and the accumulation of viral protein (35, 43). In addition, we recently showed by Western blot (immunoblot) analysis that the CNS of *ts*1-infected mice exhibits increased accumulation of gPr80*env* (23). However, virus replication per se is not sufficient to induce the overt hind limb paralysis observed in *ts*1-infected mice. We further observed that for the virus to induce full-fledged neurologic disease, two features are necessary. First, the virus must possess the ability to invade and replicate to a high titer in the CNS; second, the virus must possess neurocytopathic characteristics (28, 34, 40). By histopathological analysis, we observed that both neurovirulent *ts*1 and nonneurovirulent wild-type MoMuLV-TB (WT) induce similar lesions in corresponding areas of the CNS (43), albeit that lesions in WT-infected mice are milder and no neurologic symptoms develop. We also found that in the CNS of *ts*1-infected mice, lesions in the form of intracellular vacuolation, nuclear flocculation, and vesicular enlargement of the ER and Golgi complex prior to breakdown of the cell membrane and cellular disintegration occur in all cell types of neuroectodermal origin, i.e., astrocytes, oligodendrocytes, and neurons (27, 43), whereas no CPE is observed in microglial cells and vascular endothelial cells, although the latter apparently is the cell type among all the cell types in the CNS that is most conspicuous in virus replication and production (27). To correlate the genetically conferred properties of *ts*1 with its neurovirulence and to understand why certain cells, such as endothelial cells, are not killed by viral infection, whereas other cell types, such as astrocytes, demonstrate cytopathic changes as a result of viral infection, we recently established primary cell cultures of CNS endothelial cells and astrocytes in our laboratory to investigate the specific interaction of *ts*1 and the WT with these cells. Our results, presented in this report, showed that although *ts*1 productively replicated in primary endothelial cells and astrocytes as well as in a continuous cell line, TB, it caused pathologic changes in astrocytes only. High levels of viral expression and inefficient transport of gPr80*env*, resulting in the intracellular accumulation of gPr80*env* as well as virus particles, apparently correlated with the cytopathic alterations induced by *ts*1 in astrocytes.

MATERIALS AND METHODS

Viruses and cell lines. The isolation and molecular cloning of *ts*1 and its parental virus, MoMuLV-TB, were described previously (37, 42). Viruses were propagated in TB cells, a

* Corresponding author.

thymus-bone marrow cell line derived from CFW/D mice, and the viral titer was determined on 15F cells as previously described (39). All cell lines were maintained in Dulbecco's modified Eagle medium (DMEM) supplemented with 6% fetal calf serum and 4% bovine serum.

Primary astrocyte and endothelial cell cultures. The mouse subcortical diencephalon and brain stem were dissected from 3- to 7-day-old FVB/N mice. The tissues were minced in cold phosphate-buffered saline (PBS) on ice, triturated through 100-μm-pore-size Nitex screens and then 50-μm-pore-size sterile metal grids, and rinsed by centrifugation at 4°C for 7 min at 120 × *g* in PBS. The cells were suspended in an equal volume of 0.5% collagenase–0.2% DNase (Sigma Chemical Co., St. Louis, Mo.) and incubated with constant agitation for 20 to 25 min at 37°C. The dissociated tissue homogenate was washed twice with 2% Nu-serum (Collaborative Research, Inc., Bedford, Mass.) in PBS, placed on a 15% dextran–1% Nu-serum gradient in PBS, and spun at 4,000 × *g* for 20 min at 4°C to separate the astroglial cells (in the supernatant) from the microvascular endothelial cells (in the pellet). Cells from the supernatant and the pellet were washed separately twice as described above, placed on a 30% Percoll–1% Nu-serum or a 45% Percoll–1% Nu-serum gradient, and spun at 20,000 × *g* for 20 min at 10°C. Cells from the supernatant of the 30% gradient were washed twice, counted, and placed in gelatin-coated cell culture wells at a density of 10^4 to 10^5 cells per cm^2 in DMEM containing 20% Nu-serum, 1× BME vitamins (GIBCO, Grand Island, N.Y.), 100 U of penicillin per ml, 0.1 mg of streptomycin per ml, and 4 μg of amphotericin B (Sigma) per ml. The cells developed into enriched astroglial cell cultures after passage in vitro at 37°C in 5% CO_2. Cells from the supernatant of the 45% gradient were washed twice and placed in fibronectin-coated cell culture wells at 1×10^5 to 5×10^5 cells per cm^2 in endothelial cell growth medium, which contained DMEM; 20% Nu-serum; 150 mg of endothelial cell growth supplement (Collaborative Research) per ml; 5 μg each of insulin, transferrin, and selenium per ml; 4.4 U of heparin per ml; 0.5 mM pyruvate; 200 mM glutamine (Sigma); and BME vitamins and antibiotics as listed above. The cells developed into endothelial cell cultures after several passages.

Characterization of astrocytes and endothelial cells. The cells were characterized by alkaline phosphatase analysis, immunocytochemistry, immunoblotting, immunoprecipitation, and fluorescence-activated cell sorting as previously described (25). The antibodies used were anti-glial-fibrillary acidic protein (GFAP), anti-actin (Sigma), anti-factor VIII (Dako, Santa Barbara, Calif.), anti-neuronal enolase (a gift from D. Schmeckel), and anti-galactocerebroside (a gift from D. Silverberg). *Bandeiraea simplicifolia* isolectin B_4 (Sigma) was also used as a marker for endothelial cells. Astrocytes consistently by the fourth or fifth passage were >99% GFAP positive, >99% actin positive, <0.2% galactocerebroside positive, <0.1% neuronal enolase positive, and <0.1% factor VIII positive. By the fourth or fifth passage, endothelial cells consistently were >70% factor VIII positive, >99% actin positive, and 98% *Griffonia simplicifolia* positive. In addition, in situ hybridization demonstrated unique labeling of astrocytes with a GFAP probe (>99%) and of endothelial cells with an alkaline phosphatase probe (>99%).

Infection of cells. Primary astrocyte and endothelial cell cultures and TB cells were infected with the WT or *ts*1. Fifty thousand cells were plated in 30-mm plastic tissue culture dishes 20 h before infection. Cells were treated with 4 μg of Polybrene per ml for 2 h and then infected at a multiplicity of infection of 1 with *ts*1 or the WT. After incubation for 45 min, the cells were washed and refed with fresh medium. The cultures were maintained at 34.5°C (the permissive temperature for *ts*1), and virus production and CPEs were monitored for 5 days.

Radiolabeling of cell cultures and viruses, radioimmunoprecipitation, and SDS-PAGE. At 72 h postinfection (p.i.), *ts*1- and WT-infected cells were metabolically labeled with both [^{35}S]cysteine and [^{35}S]methionine in cysteine- and methionine-free medium for 6 h. After the cells were labeled, the virus particles were harvested from clarified culture medium by ultracentrifugation at 45,000 rpm for 90 min in a Beckman TL-100 ultracentrifuge. The cell monolayers and virus pellets were lysed with *N*-octyl-β-D-glucopyranoside (Sigma). The virus and cell lysates were immunoprecipitated with 7 μl of goat antiserum prepared against Triton-disrupted murine leukemia virus (MuLV) (Microbiological Associates, Inc., Bethesda, Md.) and incubated for 1 h at 4°C. The immune complexes were recovered on fixed *Staphylococcus aureus* (Pansorbin cells) from Calbiochem-Behring, La Jolla, Calif. Eluted immune complexes were subjected to sodium dodecyl sulfate-polyacrylamide gel electrophoresis (SDS-PAGE) as described previously (29, 38).

The apparent molecular sizes (M_rs) of the proteins were determined by plotting log M_r versus relative distance migrated (26). The ^{14}C-labeled protein molecular size standards used (Dupont, NEN Research Products, Boston, Mass.) had M_rs of 97,400 (phosphorylase *b*), 69,000 (bovine serum albumin), 46,000 (ovalbumin), 30,000 (carbonic anhydrase), and 12,300 (cytochrome *c*).

Pulse-chase analysis of gPr80^{env} processing. Metabolic labeling, pulse-chase experiments, immunoprecipitation, and SDS-PAGE were performed as described previously (29). Goat antiserum prepared against Rauscher MuLV gp69/71 was obtained from Microbiological Associates. The integrated optical density of protein bands was quantified with a Millipore Bio Image system (Bio Image Products, Ann Arbor, Mich.).

Confocal immunofluorescence microscopy. Astrocytes, endothelial cells, and TB cells were grown on chamber slides (Nunc, Inc., Naperville, Ill.) at 34.5°C at a low density so that separate individual cells could be visualized. Uninfected and infected cells (2 to 3 days p.i.) were first fixed in 3% paraformaldehyde in PBS for 3 min at room temperature and then permeabilized in *N*-2-hydroxyethylpiperazine-*N*′-2-ethanesulfonic acid (HEPES)–Triton X-100 buffer (20 mM HEPES [pH 7.4], 300 mM sucrose, 50 mM NaCl, 3 mM $MgCl_2$, 0.5% Triton X-100) for 3 min at room temperature. For indirect immunolabeling of viral *env* protein, cells were first incubated with goat anti-gp70 diluted 1:300 in PBS–2% bovine serum albumin (Sigma) (PBS-BSA) for 45 min at room temperature, then washed three times in PBS-BSA, and finally incubated with fluorescein isothiocyanate-conjugated anti-goat immunoglobulin G antibody (Sigma) (diluted 1:100 in PBS-BSA) for 45 min at room temperature. The cells were then washed an additional four or five times in PBS-BSA and mounted in 0.2% *p*-phenylenediamine–glycerol for confocal microscopy. The cells were visualized with a Meridian ACAS 570 workstation (Meridian Instruments, Okemos, Mich.) and photographed from the microscope video monitor.

Transmission EM. At 72 h p.i., the cells were fixed with 4% glutaraldehyde in PBS for 2 h and postfixed in osmium tetroxide for 1 h. The cells were then dehydrated in a graded series of ethanol and propylene oxide and embedded in a mixture of Epon 812 and Araldite 6005 resins (R. P. Cargille

Laboratories, Inc.). Thin sections were stained with uranyl acetate and lead citrate. Samples were examined with a Philips electron microscope (EM).

RESULTS

CPEs induced by *ts*1 and the WT in primary astrocyte cultures. Astrocyte cultures infected with *ts*1 or the WT were maintained at 34.5°C and monitored for morphologic changes for 5 days. Endothelial and TB cells infected with *ts*1 and the WT were used as controls to test whether the ability of these viruses to kill astrocytes in cultures was specific for astrocytes.

Cytopathologic changes, such as cell lysis and syncytium formation, first appeared in *ts*1-infected astrocytes at about 70 h p.i. and about 12 h later in WT-infected astrocytes. As shown in Fig. 1, by day 4 p.i., a number of cells in both *ts*1- and WT-infected primary astrocyte cultures had already lysed, and some multinucleated syncytia had formed. However, the CPE in WT-infected astrocytes (Fig. 1B) was less severe than that in *ts*1-infected astrocytes (Fig. 1C), with fewer lysed cells and less syncytium formation. Although multinucleated giant cells were observed in both *ts*1- and WT-infected astrocyte cultures, this morphologic change was not the major CPE that we detected. The major CPE that we observed in these cultures was cell lysis. No cytopathologic changes were observed in the uninfected primary astrocyte cultures (Fig. 1A) or in *ts*1- and WT-infected endothelial and TB cells.

To assess the severity of the virus-induced CPE, we determined the numbers of viable cells at specific times by trypan blue exclusion. In several experiments, we consistently observed fewer viable cells but more dead cells and debris in *ts*1- and WT-infected primary astrocyte cultures than in uninfected astrocyte cultures at all times. Figure 2 represents the average results from these experiments. During the first 2 days p.i., the growth curves of *ts*1- and WT-infected astrocytes were similar, and both cultures showed retardation of growth. However, by day 3 p.i., when the CPE had occurred, the number of viable *ts*1-infected astrocytes was two to three times smaller than the number of viable WT-infected astrocytes. The CPE persisted from day 3 p.i. through day 5 p.i., but not all cells experienced the CPE. *ts*1-infected endothelial cells had a higher survival rate than *ts*1-infected astrocytes (Fig. 2), although the initial rates of cell growth for both cell types were unaffected by the infection. No significant differences were observed between the growth curves of *ts*1- and WT-infected and uninfected endothelial cells. Infected or uninfected TB cells had similar growth rates, and these cells grew faster than uninfected astrocytes (Fig. 2). These results indicate that although *ts*1 and WT infections were not cytopathic in endothelial and TB cells, both *ts*1 replication and WT replication in astrocytes induced cytopathic changes with cell lysis, albeit to different degrees, and *ts*1 apparently killed more cells than WT. In addition to astrocytes isolated from FVB/N mice, we have used astrocytes isolated from BALB/c mice and have observed similar results (data not shown).

Virus replication. To test for a correlation between virus-induced CPEs and efficiency of virus replication, we compared *ts*1 and WT production in astrocyte, endothelial cell, and TB cell cultures. The kinetics of *ts*1 and WT production by astrocytes, endothelial cells, and TB cells were studied p.i. with either *ts*1 or WT. As shown in Fig. 3, both *ts*1 and WT replicated slightly better in astrocytes than in either TB cells or endothelial cells. The replication of *ts*1 in astrocytes

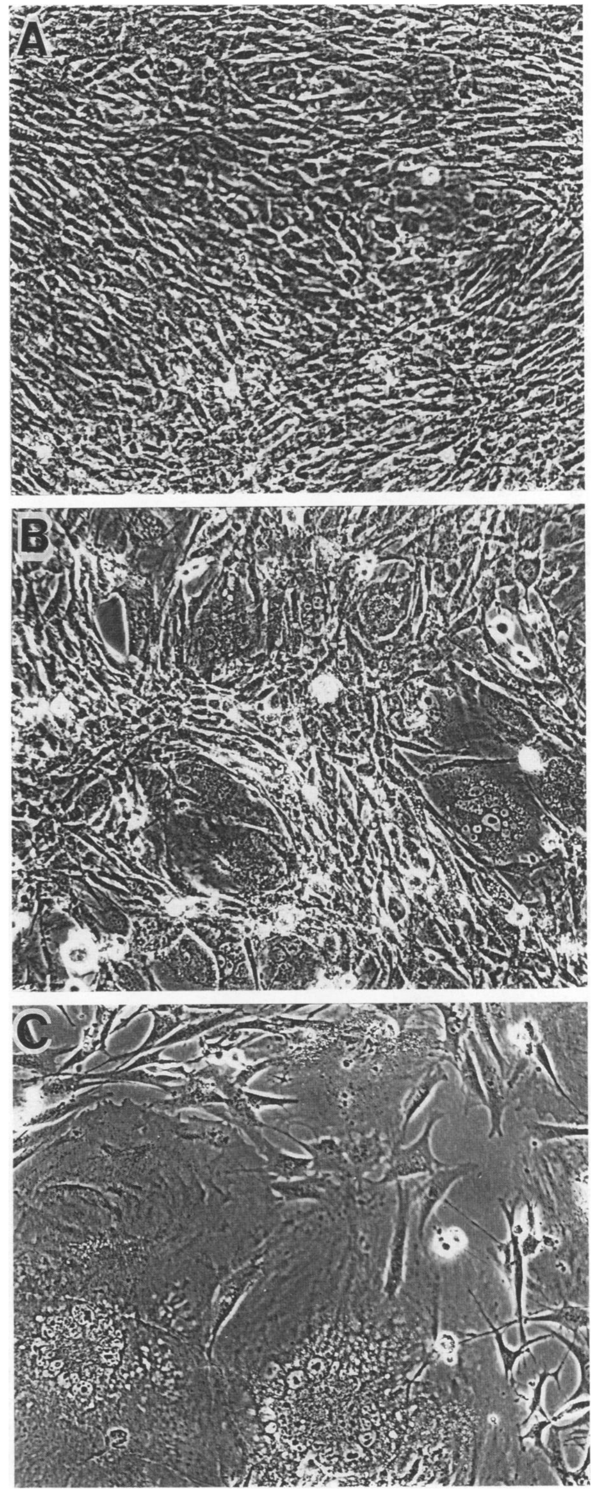

FIG. 1. CPEs in *ts*1- and WT-infected astrocytes. Cell cultures were photographed 4 days p.i. (magnification, ×40). (A) Uninfected astrocytes. (B) WT-infected astrocytes. (C) *ts*1-infected astrocytes.

was initially slower than that of WT, but by day 3 p.i., when the CPE was evident, *ts*1 production exceeded WT production in infected astrocytes or *ts*1 production in infected TB or endothelial cells. However, by day 5 p.i., virus production

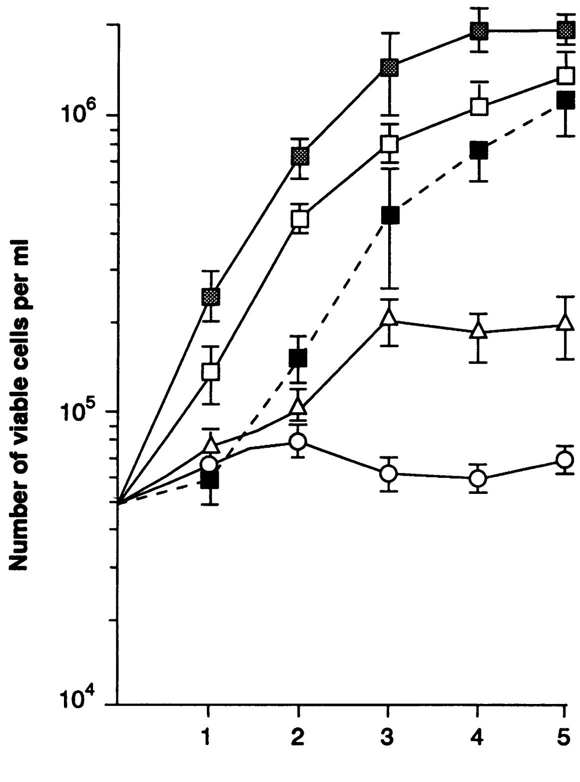

FIG. 2. Survival of cultured astrocytes after virus infection. Primary astrocyte cultures were infected with *ts*1 or the WT at a multiplicity of infection of 1. At the indicated times, viable cells in *ts*1 (○)- and WT (△)-infected astrocyte cultures were counted in a hemocytometer by trypan blue exclusion. Uninfected astrocytes (□), *ts*1-infected TB cells (▩), and *ts*1-infected endothelial cells (■) were used as controls. Data are means ± standard deviations for at least three experiments.

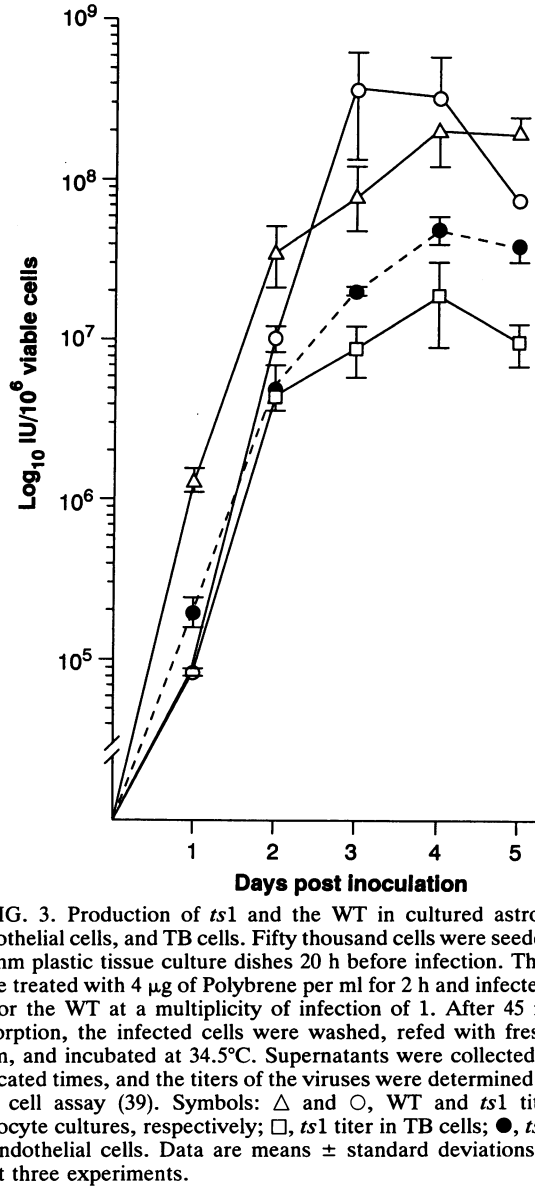

FIG. 3. Production of *ts*1 and the WT in cultured astrocytes, endothelial cells, and TB cells. Fifty thousand cells were seeded into 30-mm plastic tissue culture dishes 20 h before infection. The cells were treated with 4 μg of Polybrene per ml for 2 h and infected with *ts*1 or the WT at a multiplicity of infection of 1. After 45 min of absorption, the infected cells were washed, refed with fresh medium, and incubated at 34.5°C. Supernatants were collected at the indicated times, and the titers of the viruses were determined by the 15F cell assay (39). Symbols: △ and ○, WT and *ts*1 titers in astrocyte cultures, respectively; □, *ts*1 titer in TB cells; ●, *ts*1 titer in endothelial cells. Data are means ± standard deviations for at least three experiments.

by *ts*1-infected astrocytes was very similar to that by WT-infected astrocytes or *ts*1-infected endothelial cells.

Kinetics of gPr80^{env} processing in infected astrocytes and endothelial and TB cells. It was previously shown that *ts*1 was relatively inefficient in processing gPr80^{env} to gp70 and Prp15E (38) and that this phenotype was correlated with the neuropathologic effects of *ts*1 (28, 29). To explore the molecular basis for the cytopathic phenotype of *ts*1 in astrocyte cultures, we compared the kinetics of processing of gPr80^{env} in infected astrocytes with those in infected endothelial and TB cells. For these experiments, infected cells were radiolabeled for 10 min; this step was followed by chase periods of 0, 2, 4, and 6 h. In several experiments, our results consistently showed a higher level of synthesis but a lower efficiency of processing of gPr80^{env} in *ts*1-infected astrocytes than in *ts*1-infected TB cells. Figures 4A and B represent the results obtained from one of these experiments. Densitometric scanning of the autoradiograms showed that by the end of the 10-min labeling period, the amount of gPr80^{env} in *ts*1-infected astrocytes was 12 times higher than that in *ts*1-infected TB cells. This difference increased to 28, 50, and 88 times after 2-, 4-, and 6-h chases, respectively (compare the intensities of the protein bands in Fig. 4A). Processing of gPr80^{env} in *ts*1-infected astrocytes, compared with that in *ts*1-infected TB cells, was very inefficient. By the end of a 6-h chase, more than 80% of gPr80^{env} remained intracellularly in *ts*1-infected astrocytes (Fig. 4B). On the other hand, processing of gPr80^{env} in *ts*1-infected TB cells occurred very rapidly and efficiently, so that by the end of a 2-h chase, more than 50% of gPr80^{env} had already been processed to gp70, and by the end of a 6-h chase, only 10% of gPr80^{env} remained intracellularly (Fig. 4B).

A comparison of the kinetics of gPr80^{env} processing in *ts*1- and WT-infected astrocytes (Fig. 4C and D) showed that the processing of gPr80^{env} in the *ts*1-infected astrocytes was also less efficient than that in the WT-infected astrocytes. After a 6-h chase, 65% of gPr80^{env} remained intracellularly in *ts*1-infected astrocytes, whereas in WT-infected astrocytes, only 22% remained intracellularly. A comparison of the kinetics of gPr80^{env} processing in *ts*1-infected astrocytes and endothelial cells (Fig. 4C and E) showed that the processing of gPr80^{env} in *ts*1-infected astrocytes was also less efficient than

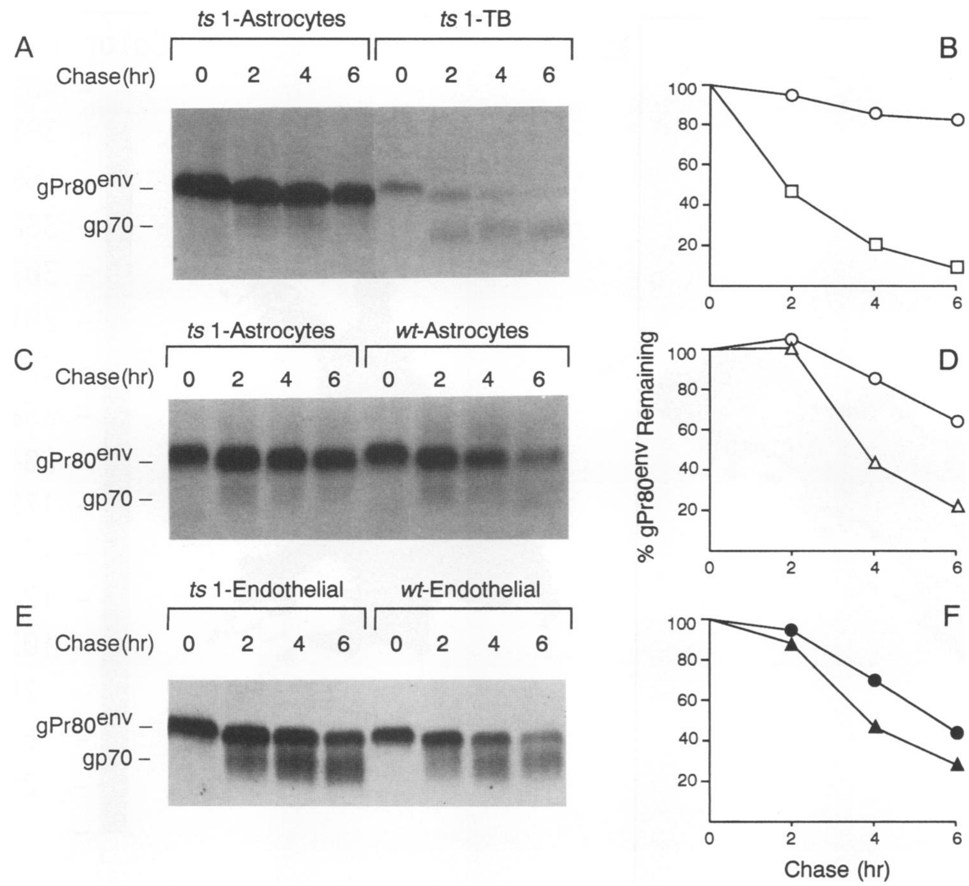

FIG. 4. Pulse-chase analysis of the processing of gPr80^{env} in *ts*1- and WT-infected cells. Astrocytes and endothelial and TB cell cultures were infected with *ts*1 or WT as described in the legend to Fig. 3. Infected cells were incubated at 34.5°C. At 2 or 3 days p.i., the same number of cells from each experiment was pulse-labeled for 10 min with both [^{35}S]cysteine and [^{35}S]methionine, and a chase was done for 0, 2, 4, and 6 h. The radiolabeled cells were lysed, and samples of the lysates containing 10^6 cpm of ^{35}S were treated with anti-gp70 antiserum. Immunoprecipitated proteins were separated by SDS-PAGE. The autoradiograms were scanned and processed by use of the Millipore Bio Image system. (A, C, and E) Autoradiograms of gPr80^{env} processing in *ts*1- or WT-infected cells. (B, D, and F) Kinetics of gPr80^{env} processing as analyzed by densitometric scanning of the autoradiograms in A, C, and E, respectively. Symbols: ○, *ts*1-infected astrocytes; □, *ts*1-infected TB cells; ●, *ts*1-infected endothelial cells; △, WT-infected astrocytes; ▲, WT-infected endothelial cells.

that in *ts*1-infected endothelial cells (see the decrease in the gPr80^{env} band intensity and the increase in the gp70 band intensity with time after chase in *ts*1-infected endothelial cells). Furthermore, the processing of *ts*1 gPr80^{env} in endothelial cells was also less efficient than the processing of WT gPr80^{env} in endothelial cells (Fig. 4E and F). Since CPEs were observed in both *ts*1- and WT-infected astrocyte cultures and not in infected endothelial and TB cells, it is possible that the accumulation of gPr80^{env} in astrocytes was related to the CPE observed in these cells. In addition, since the CPE in *ts*1-infected astrocytes was more severe than the CPE observed in WT-infected astrocytes, the pulse-chase studies provided additional evidence that the level of intracellular accumulation of gPr80^{env} was correlated with the severity of the CPE. Immunoprecipitation experiments were also performed with uninfected astrocytes and endothelial cells. We did not detect any immunoprecipitation of gPr80^{env} or gp70 in these cells.

Confocal immunofluorescence microscopy. Since the proteolytic processing of gPr80^{env} occurs in the Golgi compartment (18), it has been suggested that inefficient processing of gPr80^{env} is due to a defect in its transport from the ER to the Golgi compartment (15, 41). To obtain direct evidence for the localization of *env* proteins in the cells, we conducted a confocal immunofluorescence microscopic study of *ts*1-infected astrocytes and endothelial and TB cells. The results showed that in *ts*1-infected astrocytes, *env* proteins were located mainly near the nucleus, and relatively fewer *env* proteins were found on or near the cell surface (Fig. 5B). On the other hand, in *ts*1-infected endothelial cells, *env* proteins were distributed throughout the cell (Fig. 5A). The distribution of *env* proteins in WT-infected astrocytes was similar to that in *ts*1-infected astrocytes, albeit they were more diffused, whereas the distribution of *env* proteins in WT-infected endothelial cells was essentially the same as that in *ts*1-infected endothelial cells (data not shown). These data indicate that in astrocytes, gPr80^{env} transport from the ER was unable to keep pace with the rate of production and, as a result, unprocessed gPr80^{env} accumulated in the perinuclear region. In endothelial cells, the rates of production and transport of gPr80^{env} were more evenly balanced, and perinuclear accumulation of gPr80^{env} did not occur.

Analysis of extracellular viral proteins. To find out whether the inefficient transport and processing of intracellular *env* proteins in *ts*1- and WT-infected astrocytes could affect the extracellular protein profiles of these viruses, we examined

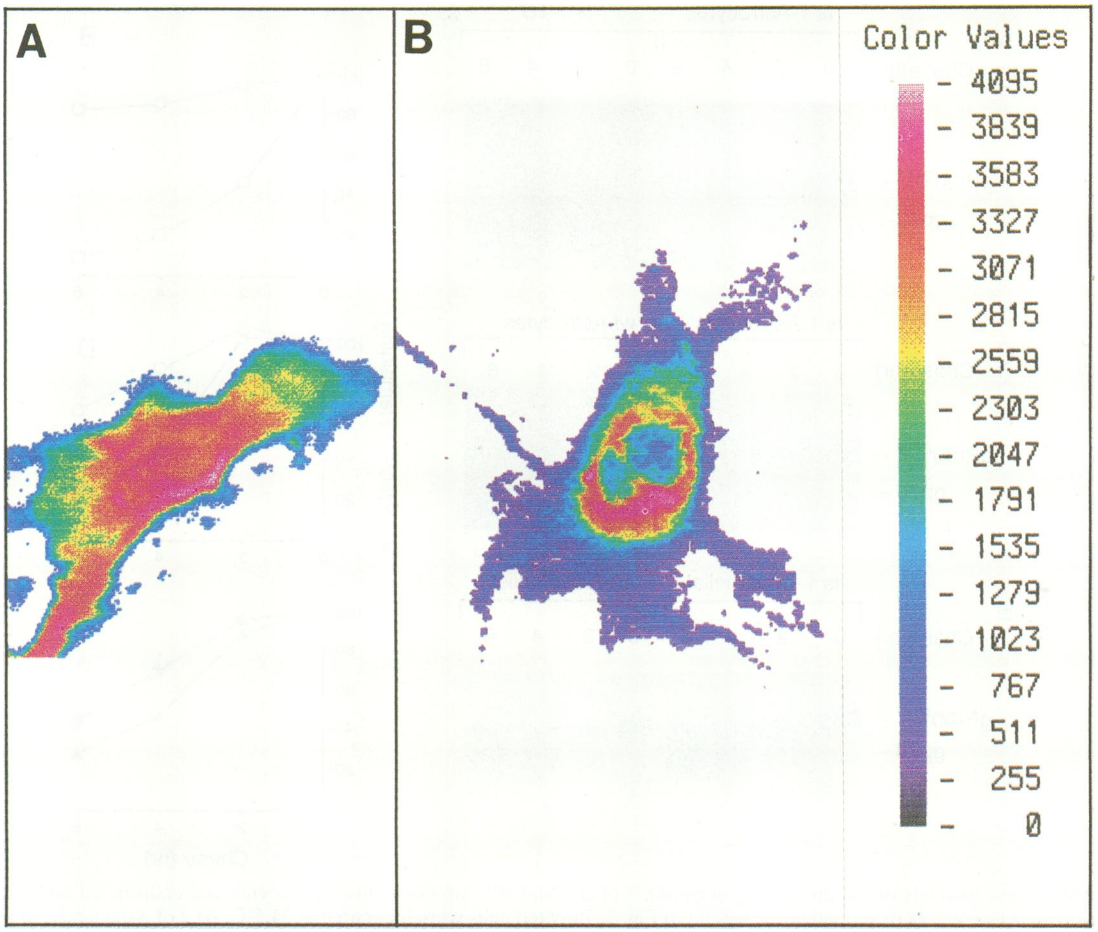

FIG. 5. Localization of viral envelope proteins in astrocytes and endothelial cells by confocal scanning microscopy. Fixed cells were incubated first with goat anti-gp70 antiserum and then with fluorescein isothiocyanate-conjugated rabbit anti-goat antibodies as described in Materials and Methods. Uninfected cells were similarly treated as controls. A microscopic field containing a single cell was selected and scanned with an argon laser at an excitation wavelength of 488 nm (scan parameters were optimized for maximum detection of fluorescence with minimum cellular photobleaching). The emitted fluorescence was detected without a barrier filter. Control cells (not shown) did not show any significant fluorescence. Ten to 20 different fields were measured and showed a similar distribution of fluorescence. (A) *ts*1-infected endothelial cell. (B) *ts*1-infected astrocyte. The color bar on the right shows the relative amount of fluorescence. A phase-control picture (not shown) confirmed the cellular outline and location of the nucleus.

the amounts of envelope proteins and p30 incorporated into the virions released from these cells. Quantitation of the amounts of proteins incorporated into extracellular virions by densitometric scanning of autoradiograms showed that both *ts*1 and WT virions released from infected astrocytes had similar amounts of p30, whereas the amounts of gp70 and p15E were about 40% lower in *ts*1 virions than in WT virions (Fig. 6, lanes 1 and 2). At the same time, analyses of the intracellular viral proteins (lanes 3 and 4) showed that there was about 40% more gPr80^{env} (but less gp70 and Prp15E) in *ts*1-infected astrocytes than in WT-infected astrocytes. No differences were found in the amounts of viral proteins of extracellular *ts*1 and WT virions produced from infected TB cells (data not shown). These results confirm our observation that the processing of gPr80^{env} to gp70 and Prp15E is less efficient in *ts*1-infected astrocytes than in WT-infected astrocytes and, as a result, relatively smaller amounts of gp70 and p15E are incorporated into the released *ts*1 virions.

Transmission EM. To determine the ultrastructural aspects of the virus-induced cytopathic changes in primary astrocyte cultures, we processed infected cells for EM examination 3 days p.i. Surprisingly, in both the *ts*1- and the WT-infected samples examined, only a few cells presented typical type C virus budding from the plasma membrane without other ultrastructural modifications. However, in most cells, virus particles were seen in dilated cisternae of the rough ER (RER) or in intracytoplasmic vacuoles (Fig. 7A). Channels of the RER were often filled with immature virus particles with aberrant shapes and forming extended tubular structures (Fig. 7B). The vacuoles contained predominantly mature particles, in a mixture of conventional and pleomorphic virus particles. It is likely that the intracellular accumulation of virus particles increased over time and thus could have contributed to the CPE observed. Such cells eventually lysed and released large numbers of virions into the medium. This result was substantiated by our ultrastructural analysis, which revealed that the largest numbers of extracellular virus particles were observed mixed with cellular debris or associated with cytoplasmic vacuoles undergoing disruption by day 3 or 4 p.i. (data not shown). Since the CPE in *ts*1-infected astrocytes was more severe than that

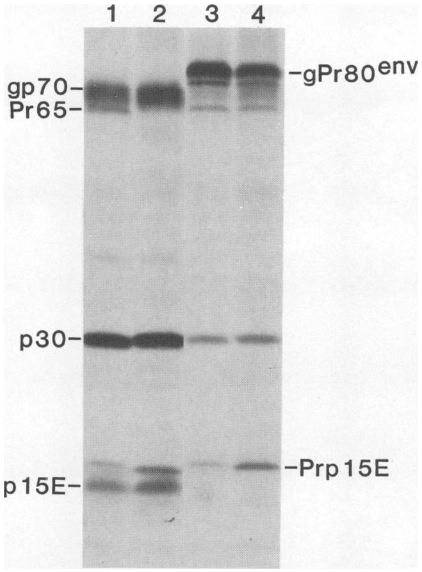

FIG. 6. Characterization of proteins in extracellular virions and cell lysates in astrocyte cultures infected with *ts*1 (lanes 1 and 3) and WT (lanes 2 and 4). At 2 or 3 days p.i., the cells were metabolically labeled with both [^{35}S]cysteine and [^{35}S]methionine for 6 h. Virus particles from the culture medium were pelleted by ultracentrifugation. Virus pellets (lanes 1 and 2) and cell monolayers (lanes 3 and 4) were compared, and samples of the lysates containing the same amount of incorporated ^{35}S were treated with anti-gp70 antiserum. Immunoprecipitated proteins were separated by SDS-PAGE. The autoradiograms were scanned and processed by use of the Millipore Bio Image system.

in WT-infected astrocytes (Fig. 1 and 2), one would expect that more intracellular virus particles would be released by cell lysis of *ts*1-infected astrocytes. This expectation may also explain our observation that the increase in the viral titer of *ts*1-infected astrocyte cultures 3 or 4 days p.i. (Fig. 3) could have been due to the release of intracellular virus particles by cell lysis together with the release of virus from the plasma membrane.

We have not specifically quantitated the numbers of intracellular virus particles in *ts*1- and WT-infected astrocytes, but our overall impression is that the number of intracellular particles was larger in *ts*1-infected astrocytes than in WT-infected astrocytes. This finding could also correlate with the more severe CPE observed in *ts*1- than in WT-infected astrocytes. No virus particles were found intracellularly or extracellularly in uninfected astrocyte cultures. To our knowledge, the activation of an endogenous virus by site-specific integration of exogenous MuLV in cell cultures has not been reported. Therefore, the intracellular particles that we observed are most likely not due to the activation of endogenous virus expression by *ts*1 or WT. Furthermore, the virus obtained from *ts*1-infected astrocytes retained the genotype as well as the phenotype of *ts*1 and was able to induce neurologic disease when inoculated into FVB/N mice (data not shown).

EM examination of *ts*1- and WT-infected endothelial and TB cells revealed typical budding type C particles on the plasma membrane (data not shown). However, in infected endothelial cells, in addition to budding particles, virus particles were also observed in intracytoplasmic vacuoles. No intracellular particles were detected in infected TB cells.

DISCUSSION

In this report, we presented evidence that the WT and its neurovirulent mutant *ts*1 not only replicated productively in primary astrocyte cultures but also directly induced CPEs in these cells, albeit to different degrees, with *ts*1 killing more cells than the WT. To our knowledge, this is the first demonstration that replicating murine retroviruses can cause pathologic changes in astrocytes in vitro. However, there are several reports indicating that human immunodeficiency virus (HIV) can also directly infect and replicate in cultured astrocytes (2–5, 8, 9). Some of these reports described mild morphologic changes in astrocytes after infection with HIV. For instance, Dewhurst and coworkers (9) detected cytoplasmic swelling and an increased number of rounded cells in highly HIV-positive glial cell lines. However, these cell lines did not undergo lysis or syncytium formation. In addition, a temporary cell growth retardation was reported for HIV-infected human astrocytic cell lines (2, 4), but no CPE developed. More recently, Volsky and coworkers (30) showed for the first time strong evidence of HIV cytopathogenicity for astrocytes in vitro, characterized by the appearance of large multinucleated syncytia and significant cytolysis. They correlated the CPE with the high efficiency of HIV replication in the CD4$^+$ glial cell line H4/CD4. In addition to HIV, feline immunodeficiency virus (FIV) has also been shown to infect and kill primary feline astrocytes (10).

The data presented here and our previous data demonstrate that *ts*1 and WT infection of other primary cell cultures, e.g., endothelial cells and macrophages (36), and of continuous cell lines, such as TB and NIH 3T3, is not cytopathic. In the study presented here, we used these cell lines as controls to investigate the mechanisms responsible for the killing of astrocytes by *ts*1 and the WT.

The overall level of virus expression, as determined by viral titers, and the amounts of gPr80^{env} and intracellular virus particles as well as viral *env* mRNA detected by in situ hybridization (Szurek, et al., unpublished data) at day 3 p.i. in *ts*1- and WT-infected astrocytes were higher than those in infected endothelial and TB cells. The higher level of virus expression in astrocytes, however, was not necessarily due to a higher growth rate of these cells, because TB cells, which had a higher growth rate (Fig. 2), expressed less virus than astrocytes (Fig. 3). Most likely, the higher viral titers obtained from *ts*1- and WT-infected astrocytes than from *ts*1- and WT-infected endothelial and TB cells were due to the large number of intracellular virus particles released into the medium upon lysis of the astrocytes at day 3 or 4 p.i.

Our results also showed a correlation between the inefficient processing of gPr80^{env} and the CPE. Processing of gPr80^{env} in *ts*1-infected astrocyte cultures was consistently less efficient than that in *ts*1-infected endothelial cells or TB cells (Fig. 4), in which no CPE was observed. The inefficient processing of gPr80^{env} in *ts*1-infected astrocytes was further substantiated by the decrease in the amounts of gp70 and p15E incorporated into the virions released (Fig. 6). Furthermore, *ts*1-infected astrocytes, which consistently showed a more severe CPE, also showed a higher level of intracellular accumulation of gPr80^{env} than WT-infected astrocytes. Confocal immunofluorescence microscopy revealed that the *env* proteins in *ts*1-infected astrocytes were mainly distributed near the nuclei, while in *ts*1-infected endothelial and TB cells, these proteins were distributed throughout the cells, indicating that the slower rate of gPr80^{env} processing in astrocytes was most likely due to inadequate transport of the protein from the ER. Using confocal immunofluorescence

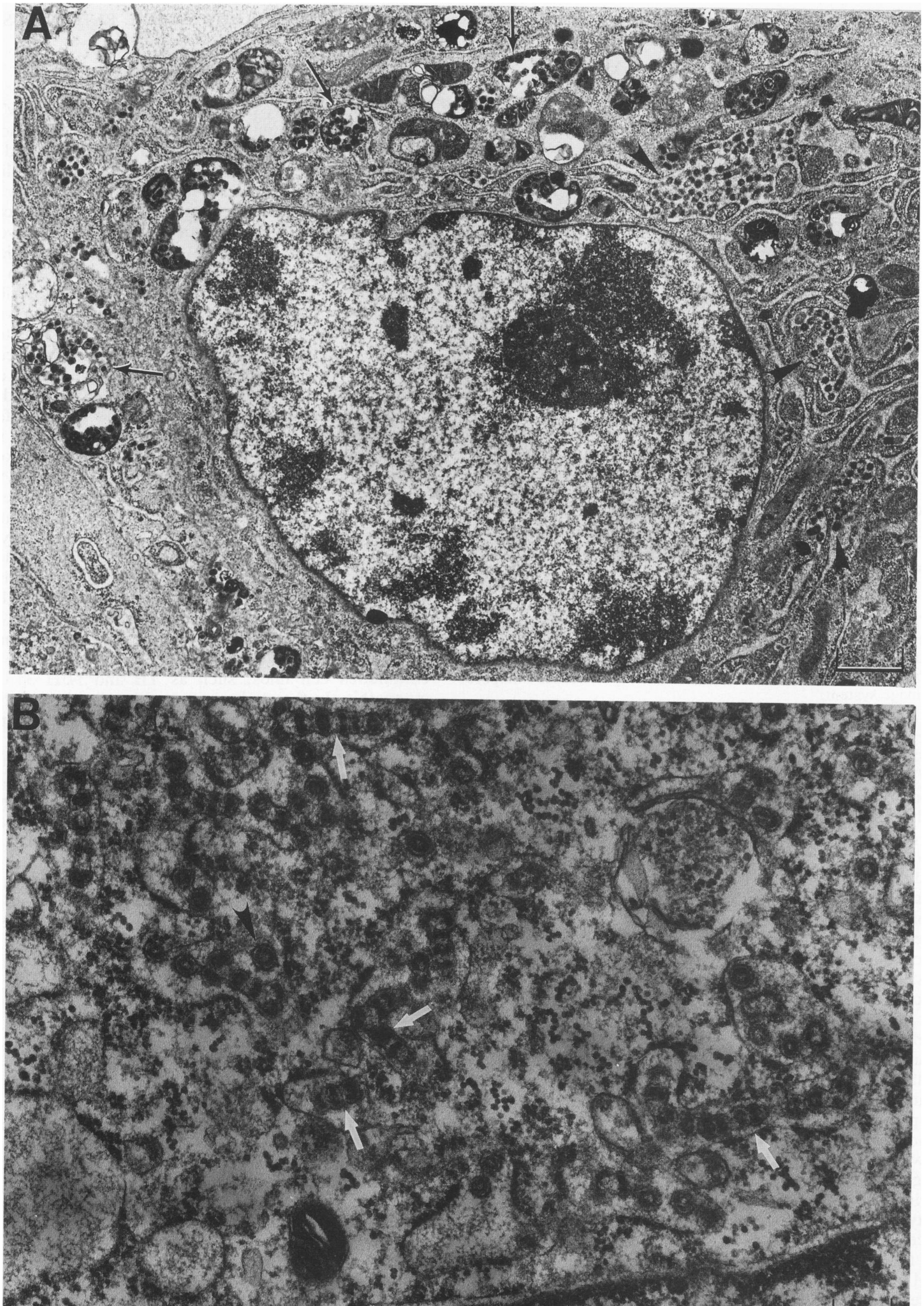

FIG. 7. Intracellular accumulation of virus particles in *ts*1-infected astrocyte cultures. (A) Electron micrograph of an astrocyte containing virus particles in cellular vacuoles (arrows) and the RER (arrowheads). Bar, 1 mm. (B) Higher-magnification micrograph of a cultured astrocyte containing aberrant virus particles (white arrows) in the RER. Bar, 0.2 mm.

microscopy, Crise and Rose (6) also showed retention of the gp160 complex in the ER of HIV type 1-infected cells. However, the mechanism responsible for retaining such proteins in the ER is not clear. A recent report by Denning et al. (7) showed that a single mutation in the cystic fibrosis transmembrane conductance regulator rendered this protein temperature sensitive in transport and, as a result, it was unable to leave the ER upon synthesis at the restrictive temperature. Interestingly, this temperature-sensitive transport-defective mutant protein is most commonly associated with cystic fibrosis. Although our previous studies demonstrated that the transport and processing of $gPr80^{env}$ in *ts*1-infected TB and NIH 3T3 cells are temperature dependent (15, 29, 38), the inefficient transport and processing of $gPr80^{env}$ in *ts*1-infected astrocyte cultures that we report here is cell type dependent, since these experiments were conducted at 34.5°C, the permissive temperature for *ts*1 replication. Other studies have also shown a strong cell type dependence for gp160 processing or transport in HIV type 1-infected cells (11, 32) or cell type-specific modifications of the FIV envelope glycoprotein (22). The study by Poss and co-workers (22) also showed that specific astrocyte killing by FIV is related to a cell type-specific modification of the envelope glycoprotein. Our findings that $gPr80^{env}$ transport and processing were consistently less efficient in *ts*1-infected astrocytes than in WT-infected astrocytes and that *ts*1-infected astrocytes showed more CPEs than WT-infected astrocytes further suggest that a direct link exists between the degree of inefficiency of $gPr80^{env}$ transport and the severity of the CPE. Our previous finding showed that a single Val→Ile substitution at position 25 in $gPr80^{env}$ is responsible for the inefficient $gPr80^{env}$ transport of *ts*1 (29). We suggested that at the restrictive temperature, the Val→Ile substitution may lead to the improper folding of $gPr80^{env}$. The misfolded $gPr80^{env}$ is not efficient for transport from the ER to the Golgi apparatus and, as a result, a pool of unprocessed $gPr80^{env}$ would remain in the ER (15, 40). It is likely that because of a specific virus-astrocyte interaction, the same mutation also causes the relatively less efficient $gPr80^{env}$ transport in *ts*1-infected astrocytes, even at the permissive temperature.

High-level virus expression together with a rate-limiting transport of $gPr80^{env}$ results in the intracellular accumulation of $gPr80^{env}$ in astrocytes. The accumulation of this viral protein can damage the astrocytes by several mechanisms. For example, the accumulation of $gPr80^{env}$ in the ER may induce dilation of the ER, resulting in the formation of cytoplasmic vacuoles, or it may physically obstruct the transport of other cellular proteins (40). It is also possible that the retention of viral *env* protein in the ER results in complex formation between the *env* protein and cellular proteins. Precursor envelope proteins of other retroviruses have been shown to bind to host cell proteins in the ER. For example, gp160 of HIV was reported to form a complex with CD4 molecules, and these complexes were retained in the ER, sometimes in close proximity to the nuclear pores (6, 16, 17). These complexes may disturb intracellular signaling or transport of many molecules between the nucleus and the cytoplasm. The intracellular accumulation of $gPr80^{env}$ may also cause congestion of traffic, resulting in the retention of other viral components. Our EM studies suggest that intracellular aberrant virus formation may also play an important role in astrocyte injury by *ts*1. It is quite possible that intracellular virus formation in astrocytes is a result of the accumulation of $gPr80^{env}$ and other viral components in vacuoles and cisternae of the ER, where *ts*1 particles, a majority in an aberrant form, were found to bud and accumulate. The intracellular accumulation of virus particles has also been induced by 1-deoxynojirimycin in NIH 3T3 cells infected with Friend mink cell focus-inducing MuLV (21). 1-Deoxynojirimycin inhibits some cellular glucosidases, resulting in the intracellular accumulation of the precursor of the envelope proteins and decreasing the level of gp70. We also speculate that the assembly of *ts*1 in astrocytes is different from that in other cell types and that it occurs at both the intracellular and the plasma membranes. Intracellular virus accumulation has been observed in HIV- and lentivirus-infected macrophages and monocytes (1, 12–14, 19, 20), often accompanied by a CPE. It is possible that the accumulation of intracellular virus particles is one of the mechanisms involved in the damage of some cell types by retroviruses.

In our in vitro findings reported in this paper and in our in vivo findings (27), we have implicated that astrocytes may play an important role in neuropathogenesis in *ts*1-infected mice. However, it is also likely that the effect of *ts*1 on astrocytes is not the only mechanism that is involved in neurologic degeneration in *ts*1-infected mice. Our argument that astrocytes may play a role in neuropathogenesis is based on the following observations. First, in the CNS of *ts*1-infected mice, cytopathologic changes in the form of cytoplasmic vacuolation have been consistently observed for astrocytes, particularly perivascular and perineuronal astrocytes. Second, using immunohistochemistry and EM (27), we were able to show that astrocytes are infected with *ts*1, albeit virus expression in these cells occurs at a much lower level than in de novo-infected astrocytes in primary cultures, as reported in this paper. Third, we were recently able to isolate astrocytes directly from *ts*1-infected mice (using methods to isolate astrocytes similar to those reported in this paper) and were able to show that they are infected with *ts*1 (unpublished data). Fourth, *ts*1 can infect a variety of cells, including all cells from neuroectodermal origins and all cells from lymphoid origins, and many other cell types, such as macrophages, megakaryocytes, and acinar, endothelial, ependymal, dendritic, and muscle cells, etc. Interestingly, only cells from neuroectodermal origins and T cells, in particular $CD4^+$ T cells, show CPEs. In two of these cell types that we were able to establish in sustained primary cell cultures, namely, astrocytes (this report) and T cells (unpublished data), we were able to correlate inefficient $gPr80^{env}$ processing with cell killing.

Astrocytes, however, may also play an indirect role in neuronal degeneration induced by *ts*1 in the CNS. Astrocytes have been shown to secrete cytokines, including tumor necrosis factor alpha and transforming growth factor beta, which are neurotoxic (24, 31). Infection and subsequent damage of astrocytes by *ts*1 may stimulate abnormal astrocytic activities and the release of these neurotoxic factors. Thus, *ts*1 infection of astrocytes may indirectly contribute to neuronal degeneration. Studies are in progress in our laboratory to determine whether infection of astrocytes by *ts*1 induces these cells to release transforming growth factor beta and/or tumor necrosis factor alpha or other cytokines. In addition, we are examining whether cytokines moderate the neuronal degeneration induced by *ts*1.

We studied *ts*1-astrocyte interactions in primary cell cultures to eliminate some of the complexities of in vivo studies of the CNS. These complexities could be due to cellular heterogeneity or to the various factors involved in cell-to-cell interactions and communication. However, the results of in vitro studies must be interpreted with caution, because the characteristics of astrocytes in cultures may not necessarily reflect their intrinsic features in vivo. For example, one major difference between in vivo and in vitro systems is the lower rate of cell growth and metabolism in the former, which may contribute to the much lower level of virus expression. The relatively low level of virus expression in astrocytes in vivo may also explain why astrocytes do not undergo multinucleated giant cell formation during *ts*1 infection in the CNS. Furthermore, the lower level and slower rate of virus expression also may explain why it takes much longer for astrocytes to be killed by *ts*1 in infected mice than in vitro.

In summary, the study reported here shows that the most important characteristics of *ts*1 infection in primary astrocyte cultures are (i) cytopathogenicity of virus infection, (ii) high levels of virus expression, (iii) inefficiency of $gPr80^{env}$ transport and processing, (iv) high concentrations of viral *env* proteins near cell nuclei, and (v) intracellular accumulation of aberrant virus particles. These characteristics may be determined by the combined effects of the mutation in the *ts*1 *env* gene and the specificity of astrocytes as a cell type. It is possible that some of these characteristics are the result of specific virus-astrocyte interactions that render the astrocytes selectively vulnerable to *ts*1 infection. This selective vulnerability of astrocytes to viral infection is intensified in the case of *ts*1 because of an intrinsic inefficiency in the transport of the precursor of the envelope protein. We believe that similar mechanisms may also be involved in the damage of astrocytes by *ts*1 in vivo. For example, in vivo, as in the in vitro studies reported here, *ts*1 replicates in both astrocytes and endothelial cells but causes a CPE in astrocytes only (27). Furthermore, both *ts*1 and the WT cause histologically similar lesions in corresponding areas of the CNS, except that the WT lesions are less severe (43). This phenomenon was also reflected in our in vitro studies, in which we showed that the CPE in *ts*1-infected astrocytes is more severe than that in WT-infected astrocytes. However, the effect of *ts*1 on astrocytes may be only one of the mechanisms of *ts*1 neuropathogenesis. Further studies both in vivo and in vitro with astrocytes and other neural cells are necessary to elucidate the mechanisms of CNS damage by *ts*1.

ACKNOWLEDGMENTS

We thank D. Hollowell and J. Vann for excellent technical assistance and Rola Barhoumi for valuable assistance with the confocal microscopy. We also thank J. K. Ball and W. Lynn for reviewing the manuscript and C. McKinley for assistance in preparing it.

This investigation was supported by Public Health Service grants CA 45124 and AI 28283 (to P.K.Y.W.), core grant 16672 from NIH (MDACC), and a grant from the Department of Veterans' Affairs (to B.R.B.).

REFERENCES

1. **Banapour, B., M. L. Marthas, R. J. Munn, and P. A. Luciw.** 1991. *In vitro* macrophage tropism of pathogenic and nonpathogenic molecular clones of simian immunodeficiency virus (SIV mac). Virology **183:**12–19.
2. **Brack-Werner, R., A. Kleinschmidt, A. Ludvigsen, W. Mellert, M. Neumann, R. Herrmann, M. C. L. Khim, A. Burny, N. Muller-Lantzsch, D. Stavrou, and V. Erfle.** 1992. Infection of human brain cells by HIV-1: restricted virus production in chronically infected human glial cell lines. AIDS **6:**273–285.
3. **Cheng-Mayer, C., J. T. Rutka, M. L. Rosenblum, T. McHugh, D. P. Stites, and J. Levy.** 1987. Human immunodeficiency virus can productively infect cultured human glial cells. Proc. Natl. Acad. Sci. USA **84:**3526–3530.
4. **Chiodi, F., S. Fuerstenberg, M. Gidlund, B. Asjo, and E. M. Fenyo.** 1987. Infection of brain-derived cells with the human immunodeficiency virus. J. Virol. **61:**1244–1247.
5. **Christofinis, G., L. Papadaki, O. Sattentau, R. Ferns, and R. Tedder.** 1987. HIV replicates in cultured human brain cells. AIDS **1:**229–234.
6. **Crise, B., and Y. K. Rose.** 1992. Human immunodeficiency virus type 1 glycoprotein precursor retains a CD4-$p56^{lck}$ complex in the endoplasmic reticulum. J. Virol. **66:**2296–2301.
7. **Denning, G. M., M. P. Anderson, J. F. Amara, J. Marshall, A. E. Smith, and M. J. Welsh.** 1992. Processing of mutant cystic fibrosis transmembrane conductance regulator is temperature-sensitive. Nature (London) **358:**761–764.
8. **Dewhurst, S., J. Bresser, M. Stevenson, K. Sakai, M. Evinger-Hodges, and D. Volsky.** 1987. Susceptibility of human glial cells to infection with human immunodeficiency virus (HIV). FEBS Lett. **213:**138–143.
9. **Dewhurst, S., K. Sakai, J. Bresser, M. Stevenson, M. Evinger-Hodges, and D. Volsky.** 1987. Persistent productive infection of human glial cells by human immunodeficiency virus (HIV) and by infectious molecular clones of HIV. J. Virol. **61:**3774–3782.
10. **Dow, S. W., M. L. Poss, and E. A. Hoover.** 1990. Feline immunodeficiency virus: a neurotropic lentivirus. J. Acquired Immune Defic. Syndr. **3:**658–668.
11. **Earl, P. L., B. Moss, and R. W. Doms.** 1991. Folding, interaction with GRP78-BiP, assembly, and transport of the human immunodeficiency virus type 1 envelope protein. J. Virol. **65:**2047–2055.
12. **Folks, T. M., S. W. Kessler, J. M. Orenstein, J. S. Justement, E. S. Jaffe, and A. S. Fauci.** 1988. Infection and replication of HIV-1 in purified progenitor cells of normal human bone marrow. Science **242:**919–922.
13. **Gendelman, H. E., O. Narayan, S. Kennedy-Stoskopf, P. G. E. Kennedy, Z. Ghotbi, Y. E. Clements, J. Stanley, and G. Pezeshkpour.** 1986. Tropism of sheep lentiviruses for monocytes: susceptibility to infection and virus gene expression increase during maturation of monocytes to macrophages. J. Virol. **58:**67–74.
14. **Gendelman, H. E., J. M. Orenstein, M. A. Martin, C. Ferrua, R. Mitra, T. Phipps, L. A. Wahl, H. C. Lane, A. S. Fauci, D. S. Burke, D. Skillman, and M. S. Meltzer.** 1988. Efficient isolation and propagation of human immunodeficiency virus on recombinant colony-stimulating factor 1-treated monocytes. J. Exp. Med. **167:**1428–1441.
15. **Kamps, C. A., Y.-C. Lin, and P. K. Y. Wong.** 1991. Oligomerization and transport of the envelope protein of Moloney murine leukemia virus-TB and of ts1, a neurovirulent temperature-sensitive mutant of MoMuLV-TB. Virology **184:**687–694.
16. **Kawamura, I., Y. Koga, N. Oh-Hori, K. Onodera, G. Kimura, and K. Nomoto.** 1989. Depletion of the surface CD4 molecule by the envelope protein of human immunodeficiency virus expressed in a human $CD4^+$ monocytoid cell line. J. Virol. **63:**3748–3754.
17. **Koga, Y., M. Sasaki, K. Naramura, G. Kimura, and K. Nomoto.** 1990. Intracellular distribution of the envelope glycoprotein of human immunodeficiency virus and its role in the production of cytopathic effect in $CD4^+$ and $CD4^-$ human cell lines. J. Virol. **64:**4661–4671.
18. **Kornfeld, R., and S. Kornfeld.** 1985. Assembly of asparagine-linked oligosaccharides. Annu. Rev. Biochem. **54:**631–664.
19. **Orenstein, J. M., M. S. Meltzer, T. Phipps, and H. E. Gendelman.** 1988. Cytoplasmic assembly and accumulation of human immunodeficiency virus types 1 and 2 in recombinant human colony-stimulating factor 1-treated human monocytes: an ultrastructural study. J. Virol. **62:**2578–2586.
20. **Pautrat, G., M. Suzan, D. Salaun, P. Corbeau, C. Allasia, G. Morel, and P. Filippi.** 1990. Human immunodeficiency virus type 1 infection of U937 cells promotes cell differentiation and a new pathway of viral assembly. Virology **179:**749–758.
21. **Pinter, A., W. J. Honnen, and Y. Soo Li.** 1984. Studies with inhibitors of oligosaccharide processing indicate a functional role for complex sugars in the transport and proteolysis of Friend mink cell focus-inducing murine leukemia virus envelope

proteins. Virology **136:**196–210.

22. **Poss, M. L., S. W. Dow, and E. A. Hoover.** 1992. Cell-specific envelope glycosylation distinguishes FIV glycoproteins produced in cytopathically and noncytopathically infected cells. Virology **188:**25–32.
23. **Saha, K., and P. K. Y. Wong.** Unpublished data.
24. **Sawada, M., N. Kondo, A. Suzumura, and T. Marunouchi.** 1989. Production of tumor necrosis factor-alpha by microglia and astrocytes in culture. Brain Res. **491:**394–397.
25. **Schreibengraber, S., R. Madden, D. Schrader, S. Bjornstad, J. M. Rozental, and B. R. Brooks.** Submitted for publication.
26. **Shapiro, A. L., E. Vinuela, and J. V. Maizel.** 1967. Molecular weight estimation of polypeptide chains by electrophoresis in SDS-polyacrylamide gels. Biochem. Biophys. Res. Commun. **28:**815–820.
27. **Stoika, G., O. Illanes, S. Tasca, and P. K. Y. Wong.** Submitted for publication.
28. **Szurek, P. F., E. Floyd, P. H. Yuen, and P. K. Y. Wong.** 1990. Site-directed mutagenesis of the codon for Ile-25 in gPr80 alters the neurovirulence of *ts*1, a mutant of Moloney murine leukemia virus TB. J. Virol. **64:**5241–5249.
29. **Szurek, P. F., P. H. Yuen, J. Ball, and P. K. Y. Wong.** 1990. A Val-25-to-Ile substitution in the envelope precursor polyprotein, gPr80^{env}, is responsible for the temperature sensitivity, inefficient processing of gPr80^{env}, and neurovirulence of *ts*1, a mutant of Moloney murine leukemia virus TB. J. Virol. **64:**467–475.
30. **Volsky, B., K. Sakai, M. M. Reddy, and D. J. Volsky.** 1992. A system for the high efficiency replication of HIV-1 in neural cells and its application to anti-viral evaluation. Virology **186:**303–308.
31. **Wahl, S. M., J. B. Allen, N. McCartney-Francis, M. C. Morganti-Kossmann, T. Kossmann, L. Ellingsworth, U. E. H. Mai, S. E. Mergenhagen, and J. M. Orenstein.** 1991. Macrophage- and astrocyte-derived transforming growth factor b as a mediator of central nervous system dysfunction in acquired immune deficiency syndrome. J. Exp. Med. **173:**981–991.
32. **Wiley, R. L., J. S. Bonifacino, B. J. Potts, M. A. Martin, and R. D. Klausuer.** 1988. Biosynthesis, cleavage, and degradation of the human immunodeficiency virus I envelope glycoprotein gp160. Proc. Natl. Acad. Sci. USA **85:**9580–9584.
33. **Wong, P. K. Y.** 1990. Moloney murine leukemia virus temperature-sensitive mutants: a model for retrovirus-induced neurologic disorders. Curr. Top. Microbiol. Immunol. **160:**29–60.
34. **Wong, P. K. Y., E. Floyd, and P. F. Szurek.** 1991. High susceptibility of FVB/N mice to the paralytic disease induced by ts1, a mutant of Moloney murine leukemia virus TB. Virology **180:**365–371.
35. **Wong, P. K. Y., C. Knupp, P. H. Yuen, M. M. Soong, J. F. Zachary, and W. A. F. Tompkins.** 1985. *ts*1, a paralytogenic mutant of Moloney murine leukemia virus TB, has an enhanced ability to replicate in the central nervous system and primary nerve cell culture. J. Virol. **55:**760–766.
36. **Wong, P. K. Y., G. Prasad, J. Hansen, and P. H. Yuen.** 1989. *ts*1, a mutant of Moloney murine leukemia virus-TB, causes both immunodeficiency and neurologic disorders in BALB/c mice. Virology **170:**450–459.
37. **Wong, P. K. Y., L. J. Russ, and J. A. McCarter.** 1973. Rapid selective procedure for isolation of spontaneous temperature-sensitive mutants of Moloney leukemia virus. Virology **51:**424–431.
38. **Wong, P. K. Y., M. M. Soong, R. MacLeod, G. E. Gallick, and P. H. Yuen.** 1983. A group of temperature-sensitive mutants of Moloney leukemia virus which is defective in cleavage of *env* precursor polypeptide in infected cells also induces hind-limb paralysis in newborn CFW/D mice. Virology **125:**513–518.
39. **Wong, P. K. Y., M. M. Soong, and P. H. Yuen.** 1981. Replication of murine leukemia virus in heterologous cells: interaction between ecotropic and xenotropic viruses. Virology **109:**366–378.
40. **Wong, P. K. Y., and P. H. Yuen.** 1992. Molecular basis of neurologic disorders induced by a mutant, *ts*1, of Moloney murine leukemia virus, p. 161–197. *In* R. P. Roos (ed.), Molecular neurovirology: pathogenesis of viral CNS infections. The Humana Press Inc., Totowa, N.J.
41. **Yu, Y., C. A. Kamps, P. H. Yuen, and P. K. Y. Wong.** 1991. Construction and characterization of expression systems for the env of *ts*1, a mutant of Moloney murine leukemia virus-TB. Virus Res. **19:**83–92.
42. **Yuen, P. H., D. Malehorn, C. Nau, M. M. Soong, and P. K. Y. Wong.** 1985. Molecular cloning of two paralytogenic, temperature-sensitive mutants, *ts*1 and *ts*7, and the parental wild-type Moloney murine leukemia virus. J. Virol. **54:**178–185.
43. **Zachary, J. F., C. J. Knupp, and P. K. Y. Wong.** 1986. Noninflammatory spongiform polioencephalomyelopathy caused by a neurotropic temperature-sensitive mutant of Moloney murine leukemia virus TB. Am. J. Pathol. **124:**457–468.